This is the peer reviewed version of the following article: Ikeda, Y., Satoh, A., Horinouchi, Y., Hamano, H., Watanabe, H., Imao, M., Imanishi, M., Zamami, Y., Takechi, K., Izawa‐Ishizawa, Y., Miyamoto, L., Hirayama, T., Nagasawa, H., Ishizawa, K., Aihara, K.‐I., Tsuchiya, K. and Tamaki, T. (2019), Iron accumulation causes impaired myogenesis correlated with MAPK signaling pathway inhibition by oxidative stress. Faseb, 33: 9551-9564, which has been published in final form at https://doi.org/10.1096/fj.201802724RR. This article may be used for non-commercial purposes in accordance with Wiley Terms and Conditions for Use of Self-Archived Versions.

Iron accumulation causes impaired myogenesis correlated with MAPK signaling pathway inhibition by oxidative stress

Yasumasa Ikeda[1*], Akiho Satoh[2*], Yuya Horinouchi[1*], Hirofumi Hamano[4], Hiroaki Watanabe[3], Mizuki Imao[2], Masaki Imanishi[4], Yoshito Zamami[3,4], Kenshi Takechi[5], Yuki Izawa-Ishizawa[1], Licht Miyamoto[2], Tasuku Hirayama[6], Hideko Nagasawa[6], Keisuke Ishizawa[3,4], Ken-ichi Aihara[7], Koichiro Tsuchiya[2], Toshiaki Tamaki[1]

[1]Department of Pharmacology, [2]Department of Medical Pharmacology, [3]Department of Clinical Pharmacology, [7]Department of Community Medicine for Diabetes and Metabolic Disorders, Institute of Biomedical Sciences, Tokushima University Graduate School, Tokushima, Japan

[4]Department of Pharmacy, [5]Clinical Trial Center for Developmental Therapeutics, Tokushima University Hospital, Tokushima, Japan

[6]Laboratory of Pharmaceutical and Medicinal Chemistry, Gifu Pharmaceutical University, Gifu, Japan

*These authors contributed equally to this work.

Corresponding author: Yasumasa Ikeda, MD, PhD

Department of Pharmacology, Institute of Biomedical Sciences, Tokushima University Graduate School,

3-18-15 Kuramoto-cho, Tokushima, 770-8503, Japan

E-mail: yasuike@tokushima-u.ac.jp

Tel: +81-88-633-7061, Fax: +81-88-633-7062

ABBREVIATIONS: CTX, cardiotoxin; MAPKs, mitogen-activated protein kinases; CKD, chronic kidney disease; SFO, saccharated ferric oxide; Myh, myosin heavy chain; FTH, ferritin heavy chain; FTL, ferritin light chain; ERK, extracellular signal-regulated kinase; HPF, Hydroxyphenyl fluorescein; DFO, deferoxamine; GA, gastrocnemius; DAPI, 4′,6-diamidino-2-phenylindole; DHE. dihydroethidium; Col1a1, collagen type I alpha 1 chain; Col1a2, collagen type I alpha 2 chain; Col3a1, collagen type III alpha 1 chain; Tgf-β1, transforming growth factor-beta 1; DCFH-DA, 2′ , 7′ -dichlorofluorescin diacetate; TBARS, thiobarbituric acid reactive substance ; MDA, malondialdehyde; ROS, reactive oxygen species; NF-κB, nuclear factor-kappa B

Abstract

Skeletal muscle atrophy is caused by disruption in the homeostatic balance of muscle degeneration and regeneration under various pathophysiological conditions. We have previously reported that iron accumulation induces skeletal muscle atrophy via a ubiquitin ligase-dependent pathway. However, the potential effect of iron accumulation on muscle regeneration remains unclear. To examine the effect of iron accumulation on myogenesis, we used a mouse model with cardiotoxin (CTX)-induced muscle regeneration *in vivo* and C2C12 mice myoblast cells *in vitro*. In mice with iron overload, the skeletal muscles exhibited increased oxidative stress and decreased expression of satellite cell markers. Following CTX-induced muscle injury, these mice also displayed delayed muscle regeneration with a decrease in the size of regenerating myofibers, reduced expression of myoblast differentiation markers, and decreased phosphorylation of mitogen-activated protein kinase signaling pathways. *In vitro*, iron overload also suppressed the differentiation of C2C12 myoblast cells, but the suppression could be reversed by superoxide scavenging using tempol. Excess iron inhibits myogenesis via oxidative stress, leading to an imbalance in skeletal muscle homeostasis.

Keywords: iron, myogenesis, oxidative stress, mitogen-activated protein kinases (MAPKs)

Introduction

Iron is an essential trace metal element. However, excess iron causes oxidative stress by catalyzing the production of highly toxic hydroxy-radicals via the Fenton reaction. Disorders, such as cardiomyopathy, hepatic failure, and diabetes, are induced by ectopic accumulation of excess iron in hereditary iron overload disorders (1). Moreover, increased iron content in the body can also be associated with many other diseases that do not fall under the domain of iron overload disorders. These include liver diseases (2), obesity (3), diabetes (4, 5), cardiovascular diseases (6, 7), and kidney diseases (8). These diseases are ameliorated by iron reduction, as shown by both clinical (9-11) and experimental studies (12-16) .

Skeletal muscle wasting, also known as sarcopenia, is caused by aging (17) and chronic disorders, such as chronic heart failure (18), chronic kidney disease (CKD) (19), diabetes (20), and metabolic disease (21), which worsen quality of life and lead to morbidity or mortality (22). In terms of the relationship between skeletal muscle and tissue iron content indicated by serum ferritin (a marker of body iron store), high iron content is associated with a decrease in skeletal muscle mass in elderly women (23). The serum ferritin level is also higher in sarcopenic obese individuals (24). Skeletal muscle mass has been shown to decrease with increased iron accumulation (25-27) due to the alterations in iron metabolism in aged rats. Direct iron administration reduces skeletal muscle mass due to elevated oxidative stress (28), and skeletal muscle atrophy,

induced by excessive iron, involves E3 ubiquitin ligase action mediated by the inactivation of Akt-FOXO3a due to oxidative stress (29).

Skeletal muscle is a highly regenerative organ in the body. The loss of muscle mass is induced by enhanced muscle degradation and by reduced muscle regeneration (30). In muscle regeneration, satellite cells are crucial in muscle growth and repair. In the process of regeneration upon muscle injury, the behavior of satellite cells is tightly regulated by several transcription factors during quiescence, proliferation, and differentiation. Pax-7 is expressed in adult quiescent satellite cells in mice (31) and human (32). In response to injury, satellite cells proliferate and activated cells express myogenic regulatory factors including myogenic differentiation 1 (*MyoD*), myogenic factor 5 (*Myf5*), and myogenin (*Myog*) (33), and Pax-7 is downregulated prior to terminal differentiation to myofibers (34). Notably, satellite cell dysfunction is seen in mouse models of aging (35, 36), diabetes (37-39), and CKD (40). and satellite cell numbers also decrease with age in humans (32, 41, 42).

The balance between muscle regeneration and degradation is important for the maintenance of muscle mass. As described above, excess iron promotes skeletal muscle degradation via activation of E3 ubiquitin ligase (29). However, whether the regenerative potential of normal skeletal muscle is altered during iron overload induced muscle wasting is unknown. In the present study, we found that excess iron accumulation suppressed skeletal muscle differentiation by suppressing the mitogen-activated protein kinase (MAPK) signaling pathway, and that the delay in

skeletal muscle differentiation was a consequence of oxidative stress induced by excess iron.

Material and methods

Materials

Saccharated ferric oxide (SFO) and cardiotoxin (CTX) were purchased from Nichi-Iko Pharmaceutical (Toyama, Japan) and A (St Louis, MO, USA), respectively. The following commercially available antibodies were used: anti-myosin heavy chain (Myh) 3 (same as embryonic Myh (eMyh)), anti-myogenin, anti-ferritin heavy chain (FTH), anti-ferritin light chain (FTL) (Santa Cruz Biotechnology, Inc., Dallas, TX), anti-phospho-p38MAPK (Thr180/Tyr182), anti-total p38MAPK, anti-phospho-p44/42 MAPK (extracellular signal-regulated kinase 1/2, ERK1/2), anti-total p44/42 MAPK (Extracellular Signal-regulated Kinase (ERK) 1/2) (Cell Signaling Technology, Danvers, MA, USA), anti-Pax-7 (Developmental Studies Hybridoma Bank, Iowa City, IA, USA), and anti-α-tubulin (Merck KGaA, Darmstadt, Germany) as a protein loading control. Hydroxyphenyl fluorescein (HPF) was purchased from Goryo chemical (Sapporo, Japan). Deferoxamine (DFO) was purchased from Sigma-Aldrich (St. Louis, Missouri, USA).

Animal preparation and procedures

All experimental procedures for mice were performed in accordance with the guidelines of the Animal Research Committee of Tokushima University Graduate

School, and the protocol was approved by the Institutional Review Board of Tokushima University Graduate School for animal protection (Permit Number: 13095). The mice were randomly divided into two groups: vehicle group and iron treatment group. Seven-week-old male C57BL/6J mice were obtained from Nippon CLEA (Tokyo, Japan) and were maintained with *ad libitum* access to water and food (Type NMF; Oriental Yeast, Tokyo, Japan). After 1 week of acclimation, to prepare a mouse model of iron overload, mice were treated once a week with intraperitoneal SFO (2 mg/200 µl/25 g mouse) or with the same volume of vehicle for four consecutive weeks (43). Aged C57BL/6J mice were 2 years old. Control young mice were 2 months old. In the type 2 diabetic mouse model, 8-week-old BKS-background *db/db* mice (diabetes) and heterozygous *db/m* mice (non-diabetes) were purchased from Nippon CLEA Japan, Inc. (Tokyo, Japan). Adenine-induced CKD model mice were prepared as previously described (44).

CTX-induced muscle injury model

A 50 µl volume of 10 µM CTX or an equal volume of phosphate buffered saline (PBS) was injected into the gastrocnemius (GA) muscles using an insulin syringe as described previously (45). On day 0, 3, 7, and 14 after CTX injection, the mice were euthanized by intraperitoneally injecting an overdose of pentobarbital, and GA muscles were removed and stored at −80°C until further use.

Cell culture

We used C2C12 myoblast cells to investigate the effect of excess iron on skeletal muscle differentiation as described previously (29). The cells were grown to sub-confluence for approximately 24–48 h, and incubated with either vehicle or iron sulphate ($FeSO_4$) for 24 h. The culture medium was replaced with a differentiation medium (DMEM) containing 2% horse serum, and incubated for the indicated durations. In some experiments, the cells were pre-treated with 100 μM tempol and 50 μM DFO for 1 h before stimulation with iron. The treatment protocol of $FeSO_4$ and tempol was determined in our previous study (29). We performed 3 to 6 well replicates per experiment and repeated each experiment at least 2 times. C2C12 myoblast cells were used until the 5th to 7th passages.

RNA extraction and evaluation of mRNA expression levels

The methods of RNA extraction, cDNA synthesis, and quantitative RT-PCR have been previously described (46). In brief, the tissues were homogenized with the Minilys beads-based homogenizer (Bertin Instruments, Montigny-le-Bretonneux, France) in RNAiso reagent (Takara Bio, Otsu, Japan). RNA extraction and cDNA synthesis were performed according to the manufacturer's instructions (PrimeScript RT reagent kit with gDNA Eraser (Perfect Real Time), Takara Bio). Quantitative RT-PCR was performed using the CFX Connect Real-Time PCR Detection System (Bio-Rad Laboratories, Hercules, CA, USA) with THUNDERBIRD® SYBR® qPCR Mix (TOYOBO Co., Ltd., Osaka, Japan). The primer sets used were: 5′-GACTCCGGATGTGGAGAAAA-3′ and 5′-GAGCACTCGGCTAATCGAAC-3

′ for *Pax-7*, 5′- AGTGAATGAGGCTTCGAGA-3′ and 5′-CAGGATCTCCACCTTGGGTA-3′ for *MyoD*, 5′-AGACGCCTGAAGAAGGTGAC-3′ and 5′-ACCTTGGGGAGTCTCTTCAA-3′ for *Myf5*, 5′-CACGATGGACGTAAGGGAGT-3′ and 5′-CCAGATGGACGTAAGGGAGT-3′ for *Myogenin*, 5′-AGAGTCTGTCAAGGCCCTGA-3′ and 5′-CAGCCTGCCTCTTGTAGGAC-3′ for *Myh3* (*embryonic Myh*), 5′-GAGCGGAGAGTACTGGATCG-3′ and 5′-GTTCGGGCTGATGTACCAGT-3′ for *collagen type I alpha 1 chain* (*Col1a1*), 5′-GTGTTCAAGGTGGCAAAGGT-3′ and 5′-GACCGAATTCACCAGGAAGA-3′ for *collagen type I alpha 2 chain* (*Col1a2*), 5′-ACCAAAAGGTGATGCTGGAC-3′ and 5′-GACCTCGTGCTCCAGTTAGC-3′ for *collagen type III alpha 1 chain* (*Col3a1*), 5′-TGAGTGGCTGTCTTTTGACG-3′ and 5′-AGCCCTGTATTCCGTCTCCT-3′ for *transforming growth factor-beta 1* (*Tgf-β1*), 5′-CTGTAACCGGATGGCAAACT-3′ and 5′-CTGTACCCACATGGCTGATG-3′ for *F4/80*, and 5′-GCTCCAAGCAGATGCAGCA-3′ and 5′-CCGGATGTGAGGCAGCAG-3′ for *36B4* (internal control). The expression levels of all target genes were normalized using *36B4* expression, and the values were compared to the control group in terms of relative fold changes.

Protein extraction and western blot analysis

Protein extraction and western blotting were performed as previously described (46). The tissue or cell samples were homogenized or sonicated in a protein lysis buffer containing inhibitors of proteinase and phosphatase, and the proteins were extracted. The extracted proteins were boiled for 5 min in Laemmli sample buffer and used for western blotting. The detected immune-reactive bands were quantified by densitometric analysis using Image J (version 1.38) software (National Institutes of Health, Bethesda, MD, USA) as described previously (47). Phosphorylation specific signals are normalized against levels of total target protein, and protein expression is normalized using tubulin as an internal loading control.

Histological analysis

GA muscles were fixed overnight in 4% paraformaldehyde at 4°C and embedded in paraffin. Sections 3 μm in thickness were prepared and stained with hematoxylin-eosin to measure the area of muscle fiber. Area measurements of at least 100 fibers were obtained for each animal from 10 randomly selected fields in five different sections. Muscle fiber area was quantified using Image J (version 1.38) software. The regenerating myofibers were indicated as myofibers with centralized nuclei. Picrosirius red staining was used for evaluating skeletal muscle fibrosis as previously described (48).

Fusion index

Forty-eight hours after the initiation of muscle differentiation, C2C12 cells were fixed with 4% paraformaldehyde for 10 min and stained with anti-Myh3 overnight at 4°C and mounted using mounting medium 4′,6-diamidino-2-phenylindole (DAPI, VECTASHIELD; Vector Laboratories, Burlingame, CA, USA). Five different fields per well were randomly selected and the number of nuclei in each myotube and the total number of nuclei in cells were counted in each field. The fusion index was calculated as the percentage of the total number of nuclei in Myh-positive cells from the total number of nuclei counted in the field.

In situ superoxide detection

Superoxide production in the skeletal muscle was detected by the dihydroethidium (DHE) staining method as described previously (29). Non-fixed frozen tissue sections were incubated with DHE in PBS (10 μM) in a dark, humidified container at room temperature for 30 min and then observed using a fluorescence microscope.

In situ *detection of labile ferrous iron and hydroxyl radicals*

Labile ferrous iron and hydroxyl radicals were detected by RhoNox-1 (49) and HPF, respectively. In brief, the frozen sections were fixed in 10% neutral formaldehyde for 1 min, washed with HBSS, and incubated with 5 μM RhoNox-1 and 5 μM HPF in a dark, humidified container at room temperature for 30 min. After washing,

the section was observed using fluorescence microscopy (46). RhoNox-1 was synthesized according to the literature procedure (49).

TBARS assay

A thiobarbituric acid reactive substance (TBARS) assay was used to measure malondialdehyde (MDA) concentration in skeletal muscles as previously described (13). The suspension of homogenized muscle tissue that was not centrifuged was used for the assay.

Measurement of oxidative stress in C2C12 myoblast cells

Intracellular reactive oxidative species were detected and quantified using 2′, 7′-dichlorofluorescin diacetate (DCFH-DA; Sigma-Aldrich) as described previously (46).

Cell viability assay

Cell proliferation was accessed using a CellTiter 96 AQueous non-radioactive cell proliferation assay kit (Promega KK, Tokyo, Japan) (46). Cytotoxicity was evaluated using a Cytotoxicity LDH Assay Kit-WST (DOJINDO LABORATORIES, Kumamoto, Japan) according to the manufacturer's instructions. Briefly, C2C12 myoblast cells were seeded in 96-well plates at a cell concentration of 1×10^4 cells per well and incubated for 24 h. When the cell growth was sub-confluent, $FeSO_4$ was added and the cells were cultured in DMEM with or without fetal bovine serum (FBS) for 24 h. The proliferation or cytotoxicity of cells was assessed with MTS assay or LDH assay

by measuring the absorbance at 490 nm using an iMARK microplate reader (Bio-Rad Laboratories).

Quantification of iron content

Iron content of tissues or cells was measured using an iron assay kit according to the manufacturer's instructions (Metallo assay LS, Metallogenics, Chiba, Japan) as described previously (29). Iron concentration was evaluated using tissue-weight or protein concentration and expressed as μg Fe per g of wet tissue or μg Fe per protein concentration.

Measurement of p38MAPK activity

The activity of p38MAPK was measured using a commercially available kit according to the manufacturer's instructions (CycLex p38 Kinase Assay/Inhibitor Screening Kit, MEDICAL and BIOLOGICAL LABORATORIES Co., Ltd., Nagoya, Japan).

Statistical analysis

Data are presented as mean ± standard deviation (mean ± SD). Mann–Whitney U test was used for comparisons between the two groups. For comparisons between more than two groups, the statistical significance of each difference was evaluated using the Kruskal–Wallis test. Statistical significance was indicated by $P < 0.05$.

Results

Iron content of skeletal muscle in mouse models of aging, diabetes, and CKD

Skeletal muscle regeneration is suppressed during muscle wasting due to aging in humans (41), in addition to diabetes (37) and CKD (40) in mice. We first evaluated iron accumulation in skeletal muscle under the above conditions using a mouse model involving aged mice (2-years-of-age), *db/db* mice (type 2 diabetic model), and CKD mice (adenine-induction), respectively. Iron content (Figure 1A), as well as FTH and FTL protein expression (Supplementary figure), were elevated in skeletal muscle with aging, diabetes, and CKD. Similar to iron content, oxidative stress was also increased in skeletal muscles with aging, diabetes, and CKD (Figure 1B). In terms of mRNA expression of satellite cell markers, *Pax-7*, *MyoD*, and *Myf5* were significantly reduced in skeletal muscles of mice with diabetes and CKD. Aged mice displayed reduced mRNA expression of *Pax-7* and *Myf5*, but not *MyoD*, in skeletal muscles (Figure 1C). Iron accumulation in skeletal muscle might cause the decline of satellite cells by increasing oxidative stress. Therefore, iron is a potential problem for impaired myogenesis in aging, diabetes, and CKD.

Effect of iron overload on skeletal muscle

To evaluate the effect of excess iron on muscle regeneration, we used mice with iron overload. The iron overload model showed that there were no differences in body weight and skeletal muscle weight between vehicle- and iron-treated mice (Table. 1). Iron content as well as the protein expression of FTH and FTL were increased in mice with iron overload (Figures 2A and B). Oxidative stress markers, such as DHE intensity and TBARS concentration, were increased in skeletal muscles of mice with

241 iron overload (Figures 2C and D). The mRNA expression of satellite cell markers *Pax-7*
242 and *MyoD* was significantly reduced in skeletal muscles of mice with iron overload
243 (Figure 2E). Similarly, the number of Pax-7 positive cells was reduced in skeletal
244 muscles of iron-treated mice (Figure 2F). However, there were no differences in muscle
245 fiber area as well as mRNA expression of atrogin-1 and MuRF1 between
246 vehicle-treated mice and iron-treated mice (Figure 2G and H).

247 *Suppressive action of iron accumulation on skeletal muscle regeneration after*
248 *CTX-induced injury*

249 To examine the effect of iron accumulation on skeletal muscle regeneration, CTX was
250 injected in the skeletal muscles of mice. The mRNA expression of myogenic
251 transcription factors *myogenin* and *Myh3* were upregulated in muscles after CTX injury.
252 However, their mRNA expression was downregulated in mice with iron overload
253 (Figure 3A). Histological analysis revealed that mice with iron overload showed
254 reduced number of regenerated muscle fibers with centralized nuclei as well as muscle
255 fiber area after CTX injury on day 7 and day 15 compared to control mice (Figures 3B
256 and C). In addition, fibrosis-related genes (*Col1a1*, *Col1a2*, *Col3a1*, and *Tgf-β1*
257 mRNA) were highly expressed in muscle of the iron-treated group at day3 or 7 and later
258 after CTX injury (Figure 3D). Collagen deposition was increased in CTX-injured
259 muscle at day 15 of iron overload as visualized in histology with picrosirius red staining.
260 On the contrary, no differences in the expression of the macrophage marker F4/80 were
261 observed in skeletal muscle between the vehicle- and iron-treated groups (data not

shown). The p38MAPK-dependent pathway plays a pivotal role in the activation of myogenic differentiation (50). Diabetic and CKD mice, not aged mice, showed the reduced phosphorylation of p38MAPK and ERK1/2 (Figure 1D and E). Phosphorylation of p38MAPK was upregulated in skeletal muscles after CTX injury on day 3, day 7 and day 14, which was suppressed by iron overload. Similar to p38MAPK, the degree of ERK1/2 phosphorylation was also lower on day 3 and 7 in CTX-injured muscle of mice with iron overload (Figure 3F).

Inhibitory action of iron on C2C12 myoblast differentiation

To examine the mechanism of inhibitory effect of iron on skeletal muscle regeneration, we used C2C12 myoblast cells. The proliferative activity of these cells was prevented by iron treatment in the presence or absence of serum in the culture media. We also tested cytotoxicity of iron by LDH assay, and iron treatment increased LDH release independent of the presence or absence of serum in the culture media (Figure 4A). C2C12 myoblast cells were differentiated with an increase in *Myh* and *myogenin* mRNA expression after transfer of cells to differentiation media, which inhibited by concomitant treatment with iron (Figures 4B). The fusion index of myotubes was also reduced by iron treatment (Figure 4C). p38MAPK phosphorylation was significantly higher in C2C12 myoblast cells treated with iron before differentiation. However, the increase in p38MAPK phosphorylation was even lower 5 and 10 min after transfer to the differentiation media in iron-loaded C2C12 myoblast cells compared with vehicle-loaded cells. ERK1/2 phosphorylation was also higher in C2C12 myoblast cells

at 10, 15, and 30 min after transfer to the differentiation media, which was suppressed in iron-loaded culture media beforehand (Figure 4D). Similar to p38MAPK phosphorylation, p38MAPK activity was increased after the changing to differentiation media. This increase was lowered by iron treatment (Figure 5F).

Involvement of oxidative stress in iron-mediated suppression of C2C12 myoblast differentiation

In C2C12 myoblast cells, oxidative stress was induced by iron overload, which was later suppressed by the superoxide scavenger tempol (Figure 5B). The iron content was also increased by iron treatment. However, tempol did not change the increased iron content (Figure 5A). Iron-induced inhibition of C2C12 myoblast differentiation, which lead to a reduction in mRNA expression of *myogenin* and *Myh* as well as decrease in fusion index, was restored by tempol pre-treatment (Figures 5C and D). Tempol partially ameliorated the reduced phosphorylation of p38MAPK and ERK1/2, which was inhibited by iron treatment 5 min or more after transfer to the differentiation medium (Figure 5E). In addition, tempol reversed the reduced p38MAPK activity with iron treatment 5 min after the change to differentiation medium (Figure 5G). In addition, DFO, an iron chelator, partly ameliorated iron-mediated inhibition of myoblast differentiation (Supplementary figure 2).

Discussion

Iron accumulation has a harmful effect on myogenesis due to oxidative stress, causing imbalance in skeletal muscle homeostasis. Presently, the suppression of skeletal muscle regeneration due to iron overload, the increment of oxidative stress in a mouse model of CTX injury, and the inhibitory action of iron on muscle differentiation were all recovered by tempol *in vitro*.

Skeletal muscle mass is determined and regulated by the coordinated balance between muscle degradation and regeneration. Disruption of this balance leads to a decrease in skeletal muscle mass, which is known as sarcopenia. Excess iron causes skeletal muscle atrophy by inducing protein degradation due to oxidative stress (28, 29). In the present study, excess iron also impaired myogenesis due to oxidative stress. Our findings suggested that iron plays a pivotal role in the loss of skeletal muscle mass through its anti-myogenesis properties.

Mice with excess iron showed reduced mRNA expression of the satellite cell markers *Pax-7* and *MyoD* in skeletal muscle under basal conditions. The activation of satellite cell markers is an important event during muscle repair and regeneration in mice (51, 52). Conversely, inactivation of these markers occurs with age or disease. The number and function of satellite cell markers are also reduced and impaired in muscles of mice with advancing age (35, 36, 53). The expression of *Pax-7* and *MyoD* is decreased in skeletal muscles of mice with CKD (40) and diabetes (37-39). In humans, satellite cell numbers and Pax-7 expression decrease in skeletal muscle with aging relative to those during youth (41, 42), and myogenic potential of satellite cells is

compromised in aging human muscle (54). Moreover, there is a decline in the capacity of muscle regeneration with increasing age in both mice and humans (55-57), suggesting skeletal muscle loss mediated by the reduction of myogenesis. We found that iron concentration was elevated and that satellite cell markers were reduced in skeletal muscles in mouse models of aging, CKD, and diabetes. Oxidative stress influences both the function and proliferation of satellite cells (58). Oxidative stress was increased in the skeletal muscle of the mouse models. Therefore, iron accumulation might augment oxidative stress and promote the decline of both satellite cell number and function, resulting in impaired muscle regeneration. Satellite cells are generally thought to be essential during muscle regeneration. A recent study has shown that expression of Pax-7 in satellite cells is lower, and the exercise-induced satellite cell response is blunted in skeletal muscle of old mice (32). On the other hand, satellite cell numbers do not decline in human muscle with aging (59), and there is no difference in the proliferative response of satellite cells between children and adults (58). There is no difference in satellite cell numbers between young and aged mice although an age-related decline in myoblast generation is seen in response to injury (60). Thus, studies of age-related decreases in satellite cell number and function have to date yielded contradictory results. Therefore, further studies are necessary for clarifying the role of satellite cells in impaired muscle regeneration and muscle loss during aging conditions, as well as in disease states such as diabetes and CKD.

CTX-injured muscle showed increased *Tgf-β1*, *Col1* and *Col3* mRNA and collagen deposition, and these were higher in mice with iron overload, resulting in the promotion of excessive fibrosis. Similar to skeletal muscle, iron causes tissue fibrosis in cardiovascular organs (15, 61), kidney (14, 62), and liver (63) in mouse disease models. The interaction between fibroblasts and satellite cells is important in the regulation of myogenesis (64). Abnormal extracellular matrix deposition and fibrosis are known to impair muscle regeneration after acute injury (65, 66). Deletion of satellite cells also enhances muscle fibrosis after CTX-injury (64). Therefore, increased fibrosis, as well as reduced satellite cell numbers, might lead to compromised myogenesis after CTX injury under iron overload.

CTX-injured muscle regeneration has been widely accepted as a valid means of investigating the mechanism of skeletal muscle regeneration and differentiation (67). Generally, the expression of *myogenin* and *Myh* are upregulated and regenerative muscle fibers with centered nuclei are seen during muscle regeneration after CTX injury (40, 68). In the present study, iron-treated mice displayed suppressed upregulation of *myogenin* and *Myh3* mRNA expression and the regenerative muscle fibers with central nuclei were reduced in injured muscle with CTX compared to vehicle-treated mice. This indicates the involvement of iron in impaired muscle regeneration. In addition, the phosphorylated levels of p38MAPK and ERK1/2 were increased in CTX-injured muscle. However, the increase in phosphorylated levels was also lowered in skeletal muscles of mice treated with excess iron. The p38MAPK signaling pathway is crucial in

364 regulating skeletal muscle gene expression at different stages of the myogenic process
365 (69). p38MAPK promotes skeletal muscle differentiation via activation of the MEF2C
366 transcription factor (50, 70). Thus, p38MAPK activation is essential for skeletal muscle
367 differentiation and regeneration. In the light of ERK1/2 action on skeletal muscle
368 differentiation, ERK1/2 activation also seems to promote skeletal muscle differentiation
369 in a similar manner along with the p38MAPK signaling pathway. Inhibition of ERK1/2
370 signaling suppresses multinucleated myotube formation and decreases the expression of
371 muscle-specific genes (*MyoD* and *myogenin*) in myoblasts after the induction of
372 differentiation (70-72). However, ERK1/2 is reportedly required for myoblast
373 proliferation, but not for differentiation (73, 74). Thus, the role of the ERK1/2 pathway
374 on skeletal muscle differentiation is still controversial and further research is needed to
375 clarify this aspect.

376 In the present study, excess iron increased ferrous iron and reactive oxygen
377 species (ROS) abundance in skeletal muscle, suggesting the occurrence of the Fenton
378 reaction under iron overload. C2C12 myoblast differentiation was impaired under iron
379 overload conditions, and the free radical scavenger tempol ameliorated iron-mediated
380 reduction of myoblast differentiation and MAPK activity, indicating the involvement of
381 excess iron-mediated oxidative stress in impaired muscle differentiation via inactivation
382 of the p38MAPK and ERK1/2 signaling pathways. We have previously shown that iron
383 reduces Akt-FOXO3a phosphorylation and that this phosphorylation is prevented by
384 tempol (29). Therefore, iron-mediated oxidative stress might be involved in the

suppression of the aforementioned kinase pathway. Previous studies have shown that oxidative stress induced by hydrogen peroxide or creatinine directly impairs muscle differentiation in C2C12 myoblast cells (75-77). Tumor necrosis factor-alpha-induced oxidative stress is involved in impaired muscle differentiation in tumor-bearing mice (78). Thus, ROS can generally cause inhibition of myogenic differentiation (75, 76, 79), and this action cannot be attributed solely to increased cell death (77). ROS can increase nuclear factor-kappa B (NF-κB) activity (75), which inhibits skeletal muscle differentiation (80, 81). Taken together, iron overload might promote ROS-mediated impaired myogenesis.

On the other hand, oxidative stress also plays an important signaling role in skeletal muscle adaptation (82). Contrary to our findings, oxidative stress induced by hydrogen peroxide activates the p38MAPK and ERK1/2 pathways through NF-κB transactivation in skeletal myoblasts (83). Therefore, the effect of oxidative stress on myogenesis has dual physiological and pathological aspects and is controversial (84). More research is necessary to further elucidate the inhibitory mechanisms of iron on myogenesis.

Iron deficiency is an acknowledged concern, and functional foods amended with iron are commercially available to prevent iron deficiency. However, as previously mentioned, the iron content in the human body increases with age and in diseases, including diabetes and CKD, indicating increased iron content in skeletal muscle. The level of iron intake is important. Excess iron intake impairs regeneration of skeletal

muscle and can induce muscle atrophy. Muscle atrophy and degradation in the presence of excess iron also involves the oxidative stress-ubiquitin ligase E3 pathway (29). Thus, iron deficiency and excess can be detrimental.

In conclusion, iron overload affects skeletal muscle differentiation, possibly through oxidative stress-dependent inhibition of the p38 MAPK and ERK1/2 signaling pathways. This finding suggests a crucial role of iron in muscle regeneration, and clarifies the underlying mechanisms of skeletal muscle homeostasis.

Acknowledgements

This work was supported by Japan Society for the Promotion of Science (JSPS) KAKENHI Grant (No. 15K01716 and 18K08480 to Y.I). We appreciate the excellent technical advice by the Support Centre for Advanced Medical Sciences, Institute of Biomedical Sciences, Tokushima University Graduate School. We would like to thank Editage (www.editage.jp) for their help with English language editing.

Conflict of Interest Statement

The authors declare no conflict of interests.

Author Contributions

Y.Ikeda designed research; Y.Ikeda, A. Satoh, Y. Horinouchi, H. Hamano, H. Watanabe, and M. Imao performed research; Y. Ikeda, A. Satoh, Y. Horinouchi, M. Imanishi, Y. Zamami, K. Takechi, Y. Izawa-Ishizawa, L. Miyamoto, K. Ishizawa, K. Aihara, K. Tsuchiya, and T. Tamaki analyzed data and contributed to discussion; T. Hirayama and H. Nagasawa contributed a new reagent; and Y. Ikeda and A. Satoh wrote the paper.

References

1. Camaschella, C. (2005) Understanding iron homeostasis through genetic analysis of hemochromatosis and related disorders. *Blood* **106**, 3710-3717
2. Hayashi, H., Takikawa, T., Nishimura, N., and Yano, M. (1995) Serum aminotransferase levels as an indicator of the effectiveness of venesection for chronic hepatitis C. *J Hepatol* **22**, 268-271
3. Iwasaki, T., Nakajima, A., Yoneda, M., Yamada, Y., Mukasa, K., Fujita, K., Fujisawa, N., Wada, K., and Terauchi, Y. (2005) Serum ferritin is associated with visceral fat area and subcutaneous fat area. *Diabetes Care* **28**, 2486-2491
4. Ford, E. S., and Cogswell, M. E. (1999) Diabetes and serum ferritin concentration among U.S. adults. *Diabetes Care* **22**, 1978-1983
5. Lee, D. H., Liu, D. Y., Jacobs, D. R., Jr., Shin, H. R., Song, K., Lee, I. K., Kim, B., and Hider, R. C. (2006) Common presence of non-transferrin-bound iron among patients with type 2 diabetes. *Diabetes Care* **29**, 1090-1095
6. Salonen, J. T., Nyyssonen, K., Korpela, H., Tuomilehto, J., Seppanen, R., and Salonen, R. (1992) High stored iron levels are associated with excess risk of myocardial infarction in eastern Finnish men. *Circulation* **86**, 803-811
7. Menke, A., Fernandez-Real, J. M., Muntner, P., and Guallar, E. (2009) The association of biomarkers of iron status with peripheral arterial disease in US adults. *BMC Cardiovasc Disord* **9**, 34
8. Nakanishi, T., Kuragano, T., Nanami, M., Otaki, Y., Nonoguchi, H., and Hasuike, Y. (2010) Importance of ferritin for optimizing anemia therapy in chronic kidney disease. *American journal of nephrology* **32**, 439-446
9. Hayashi, H., Takikawa, T., Nishimura, N., Yano, M., Isomura, T., and Sakamoto, N. (1994) Improvement of serum aminotransferase levels after phlebotomy in patients with chronic active hepatitis C and excess hepatic iron. *Am J Gastroenterol* **89**, 986-988
10. Fernandez, E., Blanco, C., Garcia, S., Dieguez, A., Riestra, S., and Rodrigo, L. (2005) Use of low concentrations of human IgA anti-tissue transglutaminase to rule out selective IgA deficiency in patients with suspected celiac disease. *Clin Chem* **51**, 1014-1016

11. Houschyar, K. S., Ludtke, R., Dobos, G. J., Kalus, U., Broecker-Preuss, M., Rampp, T., Brinkhaus, B., and Michalsen, A. (2012) Effects of phlebotomy-induced reduction of body iron stores on metabolic syndrome: results from a randomized clinical trial. *BMC Med* **10**, 54
12. Tajima, S., Ikeda, Y., Sawada, K., Yamano, N., Horinouchi, Y., Kihira, Y., Ishizawa, K., Izawa-Ishizawa, Y., Kawazoe, K., Tomita, S., Minakuchi, K., Tsuchiya, K., and Tamaki, T. (2012) Iron reduction by deferoxamine leads to amelioration of adiposity via the regulation of oxidative stress and inflammation in obese and type 2 diabetes KKAy mice. *Am J Physiol Endocrinol Metab* **302**, E77-86
13. Ikeda, Y., Enomoto, H., Tajima, S., Izawa-Ishizawa, Y., Kihira, Y., Ishizawa, K., Tomita, S., Tsuchiya, K., and Tamaki, T. (2013) Dietary iron restriction inhibits progression of diabetic nephropathy in db/db mice. *American journal of physiology. Renal physiology* **304**, F1028-1036
14. Ikeda, Y., Horinouchi, Y., Hamano, H., Hirayama, T., Kishi, S., Izawa-Ishizawa, Y., Imanishi, M., Zamami, Y., Takechi, K., Miyamoto, L., Ishizawa, K., Aihara, K. I., Nagasawa, H., Tsuchiya, K., and Tamaki, T. (2017) Dietary iron restriction alleviates renal tubulointerstitial injury induced by protein overload in mice. *Sci Rep* **7**, 10621
15. Naito, Y., Hirotani, S., Sawada, H., Akahori, H., Tsujino, T., and Masuyama, T. (2011) Dietary iron restriction prevents hypertensive cardiovascular remodeling in dahl salt-sensitive rats. *Hypertension* **57**, 497-504
16. Sawada, H., Hao, H., Naito, Y., Oboshi, M., Hirotani, S., Mitsuno, M., Miyamoto, Y., Hirota, S., and Masuyama, T. (2015) Aortic iron overload with oxidative stress and inflammation in human and murine abdominal aortic aneurysm. *Arterioscler Thromb Vasc Biol* **35**, 1507-1514
17. Evans, W. J. (1995) What is sarcopenia? *The journals of gerontology. Series A, Biological sciences and medical sciences* **50 Spec No**, 5-8
18. Fulster, S., Tacke, M., Sandek, A., Ebner, N., Tschope, C., Doehner, W., Anker, S. D., and von Haehling, S. (2013) Muscle wasting in patients with chronic heart failure: results from the studies investigating co-morbidities aggravating heart failure (SICA-HF). *European heart journal* **34**, 512-519

19. Mak, R. H., Ikizler, A. T., Kovesdy, C. P., Raj, D. S., Stenvinkel, P., and Kalantar-Zadeh, K. (2011) Wasting in chronic kidney disease. *Journal of cachexia, sarcopenia and muscle* **2**, 9-25
20. Kim, T. N., Park, M. S., Yang, S. J., Yoo, H. J., Kang, H. J., Song, W., Seo, J. A., Kim, S. G., Kim, N. H., Baik, S. H., Choi, D. S., and Choi, K. M. (2010) Prevalence and determinant factors of sarcopenia in patients with type 2 diabetes: the Korean Sarcopenic Obesity Study (KSOS). *Diabetes Care* **33**, 1497-1499
21. Lim, S., Kim, J. H., Yoon, J. W., Kang, S. M., Choi, S. H., Park, Y. J., Kim, K. W., Lim, J. Y., Park, K. S., and Jang, H. C. (2010) Sarcopenic obesity: prevalence and association with metabolic syndrome in the Korean Longitudinal Study on Health and Aging (KLoSHA). *Diabetes Care* **33**, 1652-1654
22. Lynch, G. S. (2001) Therapies for improving muscle function in neuromuscular disorders. *Exercise and sport sciences reviews* **29**, 141-148
23. Kim, T. H., Hwang, H. J., and Kim, S. H. (2014) Relationship between serum ferritin levels and sarcopenia in Korean females aged 60 years and older using the fourth Korea National Health and Nutrition Examination Survey (KNHANES IV-2, 3), 2008-2009. *PloS one* **9**, e90105
24. Chung, J. Y., Kang, H. T., Lee, D. C., Lee, H. R., and Lee, Y. J. (2013) Body composition and its association with cardiometabolic risk factors in the elderly: a focus on sarcopenic obesity. *Archives of gerontology and geriatrics* **56**, 270-278
25. Altun, M., Edstrom, E., Spooner, E., Flores-Moralez, A., Bergman, E., Tollet-Egnell, P., Norstedt, G., Kessler, B. M., and Ulfhake, B. (2007) Iron load and redox stress in skeletal muscle of aged rats. *Muscle & nerve* **36**, 223-233
26. DeRuisseau, K. C., Park, Y. M., DeRuisseau, L. R., Cowley, P. M., Fazen, C. H., and Doyle, R. P. (2013) Aging-related changes in the iron status of skeletal muscle. *Experimental gerontology* **48**, 1294-1302
27. Xu, J., Knutson, M. D., Carter, C. S., and Leeuwenburgh, C. (2008) Iron accumulation with age, oxidative stress and functional decline. *PloS one* **3**, e2865

28. Reardon, T. F., and Allen, D. G. (2009) Iron injections in mice increase skeletal muscle iron content, induce oxidative stress and reduce exercise performance. *Experimental physiology* **94**, 720-730
29. Ikeda, Y., Imao, M., Satoh, A., Watanabe, H., Hamano, H., Horinouchi, Y., Izawa-Ishizawa, Y., Kihira, Y., Miyamoto, L., Ishizawa, K., Tsuchiya, K., and Tamaki, T. (2016) Iron-induced skeletal muscle atrophy involves an Akt-forkhead box O3-E3 ubiquitin ligase-dependent pathway. *Journal of trace elements in medicine and biology : organ of the Society for Minerals and Trace Elements* **35**, 66-76
30. Phillips, S. M., Glover, E. I., and Rennie, M. J. (2009) Alterations of protein turnover underlying disuse atrophy in human skeletal muscle. *J Appl Physiol (1985)* **107**, 645-654
31. Seale, P., Sabourin, L. A., Girgis-Gabardo, A., Mansouri, A., Gruss, P., and Rudnicki, M. A. (2000) Pax7 is required for the specification of myogenic satellite cells. *Cell* **102**, 777-786
32. Moore, D. R., McKay, B. R., Tarnopolsky, M. A., and Parise, G. (2018) Blunted satellite cell response is associated with dysregulated IGF-1 expression after exercise with age. *Eur J Appl Physiol* **118**, 2225-2231
33. Cornelison, D. D., and Wold, B. J. (1997) Single-cell analysis of regulatory gene expression in quiescent and activated mouse skeletal muscle satellite cells. *Dev Biol* **191**, 270-283
34. Olguin, H. C., Yang, Z., Tapscott, S. J., and Olwin, B. B. (2007) Reciprocal inhibition between Pax7 and muscle regulatory factors modulates myogenic cell fate determination. *J Cell Biol* **177**, 769-779
35. Gibson, M. C., and Schultz, E. (1983) Age-related differences in absolute numbers of skeletal muscle satellite cells. *Muscle & nerve* **6**, 574-580
36. Brack, A. S., Conboy, M. J., Roy, S., Lee, M., Kuo, C. J., Keller, C., and Rando, T. A. (2007) Increased Wnt signaling during aging alters muscle stem cell fate and increases fibrosis. *Science* **317**, 807-810
37. Fu, X., Zhu, M., Zhang, S., Foretz, M., Viollet, B., and Du, M. (2016) Obesity Impairs Skeletal Muscle Regeneration Through Inhibition of AMPK. *Diabetes* **65**, 188-200

38. D'Souza, D. M., Zhou, S., Rebalka, I. A., MacDonald, B., Moradi, J., Krause, M. P., Al-Sajee, D., Punthakee, Z., Tarnopolsky, M. A., and Hawke, T. J. (2016) Decreased Satellite Cell Number and Function in Humans and Mice With Type 1 Diabetes Is the Result of Altered Notch Signaling. *Diabetes* **65**, 3053-3061
39. Fujimaki, S., Wakabayashi, T., Asashima, M., Takemasa, T., and Kuwabara, T. (2016) Treadmill running induces satellite cell activation in diabetic mice. *Biochem Biophys Rep* **8**, 6-13
40. Zhang, L., Wang, X. H., Wang, H., Du, J., and Mitch, W. E. (2010) Satellite cell dysfunction and impaired IGF-1 signaling cause CKD-induced muscle atrophy. *J Am Soc Nephrol* **21**, 419-427
41. Renault, V., Thornell, L. E., Eriksson, P. O., Butler-Browne, G., and Mouly, V. (2002) Regenerative potential of human skeletal muscle during aging. *Aging Cell* **1**, 132-139
42. Verdijk, L. B., Koopman, R., Schaart, G., Meijer, K., Savelberg, H. H., and van Loon, L. J. (2007) Satellite cell content is specifically reduced in type II skeletal muscle fibers in the elderly. *Am J Physiol Endocrinol Metab* **292**, E151-157
43. Kuo, K. L., Hung, S. C., Lee, T. S., and Tarng, D. C. (2014) Iron sucrose accelerates early atherogenesis by increasing superoxide production and upregulating adhesion molecules in CKD. *J Am Soc Nephrol* **25**, 2596-2606
44. Hamano, H., Ikeda, Y., Watanabe, H., Horinouchi, Y., Izawa-Ishizawa, Y., Imanishi, M., Zamami, Y., Takechi, K., Miyamoto, L., Ishizawa, K., Tsuchiya, K., and Tamaki, T. (2018) The uremic toxin indoxyl sulfate interferes with iron metabolism by regulating hepcidin in chronic kidney disease. *Nephrol Dial Transplant* **33**, 586-597
45. Zeng, L., Akasaki, Y., Sato, K., Ouchi, N., Izumiya, Y., and Walsh, K. (2010) Insulin-like 6 is induced by muscle injury and functions as a regenerative factor. *J Biol Chem* **285**, 36060-36069
46. Oshima, K., Ikeda, Y., Horinouchi, Y., Watanabe, H., Hamano, H., Kihira, Y., Kishi, S., Izawa-Ishizawa, Y., Miyamoto, L., Hirayama, T., Nagasawa, H., Ishizawa, K., Tsuchiya, K., and Tamaki, T. (2017) Iron suppresses erythropoietin expression via oxidative stress-dependent hypoxia-inducible factor-2 alpha inactivation. *Laboratory investigation; a journal of technical methods and pathology* **97**, 555-566

47. Gassmann, M., Grenacher, B., Rohde, B., and Vogel, J. (2009) Quantifying Western blots: pitfalls of densitometry. *Electrophoresis* **30**, 1845-1855
48. Horinouchi, Y., Ikeda, Y., Fukushima, K., Imanishi, M., Hamano, H., Izawa-Ishizawa, Y., Zamami, Y., Takechi, K., Miyamoto, L., Fujino, H., Ishizawa, K., Tsuchiya, K., and Tamaki, T. (2018) Renoprotective effects of a factor Xa inhibitor: fusion of basic research and a database analysis. *Sci Rep* **8**, 10858
49. Hirayama, T., Okuda, T., and Nagasawa, H. (2013) A highly selective turn-on fluorescent probe fro iron(II) to visualize labile iron in living cells. *Chem Sci* **4**, 1250-1256
50. Zetser, A., Gredinger, E., and Bengal, E. (1999) p38 mitogen-activated protein kinase pathway promotes skeletal muscle differentiation. Participation of the Mef2c transcription factor. *J Biol Chem* **274**, 5193-5200
51. Lepper, C., Partridge, T. A., and Fan, C. M. (2011) An absolute requirement for Pax7-positive satellite cells in acute injury-induced skeletal muscle regeneration. *Development* **138**, 3639-3646
52. Cooper, R. N., Tajbakhsh, S., Mouly, V., Cossu, G., Buckingham, M., and Butler-Browne, G. S. (1999) In vivo satellite cell activation via Myf5 and MyoD in regenerating mouse skeletal muscle. *J Cell Sci* **112 (Pt 17)**, 2895-2901
53. Gallegly, J. C., Turesky, N. A., Strotman, B. A., Gurley, C. M., Peterson, C. A., and Dupont-Versteegden, E. E. (2004) Satellite cell regulation of muscle mass is altered at old age. *J Appl Physiol (1985)* **97**, 1082-1090
54. Corbu, A., Scaramozza, A., Badiali-DeGiorgi, L., Tarantino, L., Papa, V., Rinaldi, R., D'Alessandro, R., Zavatta, M., Laus, M., Lattanzi, G., and Cenacchi, G. (2010) Satellite cell characterization from aging human muscle. *Neurol Res* **32**, 63-72
55. Cartee, G. D. (1995) What insights into age-related changes in skeletal muscle are provided by animal models? *The journals of gerontology. Series A, Biological sciences and medical sciences* **50 Spec No**, 137-141
56. Grounds, M. D. (1998) Age-associated changes in the response of skeletal muscle cells to exercise and regeneration. *Ann N Y Acad Sci* **854**, 78-91
57. Bross, R., Storer, T., and Bhasin, S. (1999) Aging and Muscle Loss. *Trends Endocrinol Metab* **10**, 194-198

58. Renault, V., Thornell, L. E., Butler-Browne, G., and Mouly, V. (2002) Human skeletal muscle satellite cells: aging, oxidative stress and the mitotic clock. *Experimental gerontology* **37**, 1229-1236

59. Roth, S. M., Martel, G. F., Ivey, F. M., Lemmer, J. T., Metter, E. J., Hurley, B. F., and Rogers, M. A. (2000) Skeletal muscle satellite cell populations in healthy young and older men and women. *Anat Rec* **260**, 351-358

60. Conboy, I. M., Conboy, M. J., Smythe, G. M., and Rando, T. A. (2003) Notch-mediated restoration of regenerative potential to aged muscle. *Science* **302**, 1575-1577

61. Ishizaka, N., Saito, K., Mitani, H., Yamazaki, I., Sata, M., Usui, S., Mori, I., Ohno, M., and Nagai, R. (2002) Iron overload augments angiotensin II-induced cardiac fibrosis and promotes neointima formation. *Circulation* **106**, 1840-1846

62. Ikeda, Y., Ozono, I., Tajima, S., Imao, M., Horinouchi, Y., Izawa-Ishizawa, Y., Kihira, Y., Miyamoto, L., Ishizawa, K., Tsuchiya, K., and Tamaki, T. (2014) Iron chelation by deferoxamine prevents renal interstitial fibrosis in mice with unilateral ureteral obstruction. *PloS one* **9**, e89355

63. Halliday, J. W., and Searle, J. (1996) Hepatic iron deposition in human disease and animal models. *Biometals* **9**, 205-209

64. Murphy, M. M., Lawson, J. A., Mathew, S. J., Hutcheson, D. A., and Kardon, G. (2011) Satellite cells, connective tissue fibroblasts and their interactions are crucial for muscle regeneration. *Development* **138**, 3625-3637

65. Sato, K., Li, Y., Foster, W., Fukushima, K., Badlani, N., Adachi, N., Usas, A., Fu, F. H., and Huard, J. (2003) Improvement of muscle healing through enhancement of muscle regeneration and prevention of fibrosis. *Muscle & nerve* **28**, 365-372

66. Li, Y., Foster, W., Deasy, B. M., Chan, Y., Prisk, V., Tang, Y., Cummins, J., and Huard, J. (2004) Transforming growth factor-beta1 induces the differentiation of myogenic cells into fibrotic cells in injured skeletal muscle: a key event in muscle fibrogenesis. *Am J Pathol* **164**, 1007-1019

67. Charge, S. B., and Rudnicki, M. A. (2004) Cellular and molecular regulation of muscle regeneration. *Physiol Rev* **84**, 209-238

68. Yoshida, T., Galvez, S., Tiwari, S., Rezk, B. M., Semprun-Prieto, L., Higashi, Y., Sukhanov, S., Yablonka-Reuveni, Z., and Delafontaine, P. (2013)

Angiotensin II inhibits satellite cell proliferation and prevents skeletal muscle regeneration. *J Biol Chem* **288**, 23823-23832

69. Lluis, F., Perdiguero, E., Nebreda, A. R., and Munoz-Canoves, P. (2006) Regulation of skeletal muscle gene expression by p38 MAP kinases. *Trends Cell Biol* **16**, 36-44
70. Wu, Z., Woodring, P. J., Bhakta, K. S., Tamura, K., Wen, F., Feramisco, J. R., Karin, M., Wang, J. Y., and Puri, P. L. (2000) p38 and extracellular signal-regulated kinases regulate the myogenic program at multiple steps. *Mol Cell Biol* **20**, 3951-3964
71. Sarbassov, D. D., Jones, L. G., and Peterson, C. A. (1997) Extracellular signal-regulated kinase-1 and -2 respond differently to mitogenic and differentiative signaling pathways in myoblasts. *Mol Endocrinol* **11**, 2038-2047
72. Gredinger, E., Gerber, A. N., Tamir, Y., Tapscott, S. J., and Bengal, E. (1998) Mitogen-activated protein kinase pathway is involved in the differentiation of muscle cells. *J Biol Chem* **273**, 10436-10444
73. Rommel, C., Clarke, B. A., Zimmermann, S., Nunez, L., Rossman, R., Reid, K., Moelling, K., Yancopoulos, G. D., and Glass, D. J. (1999) Differentiation stage-specific inhibition of the Raf-MEK-ERK pathway by Akt. *Science* **286**, 1738-1741
74. Jones, N. C., Fedorov, Y. V., Rosenthal, R. S., and Olwin, B. B. (2001) ERK1/2 is required for myoblast proliferation but is dispensable for muscle gene expression and cell fusion. *J Cell Physiol* **186**, 104-115
75. Ardite, E., Barbera, J. A., Roca, J., and Fernandez-Checa, J. C. (2004) Glutathione depletion impairs myogenic differentiation of murine skeletal muscle C2C12 cells through sustained NF-kappaB activation. *Am J Pathol* **165**, 719-728
76. Hansen, J. M., Klass, M., Harris, C., and Csete, M. (2007) A reducing redox environment promotes C2C12 myogenesis: implications for regeneration in aged muscle. *Cell Biol Int* **31**, 546-553
77. Sestili, P., Barbieri, E., Martinelli, C., Battistelli, M., Guescini, M., Vallorani, L., Casadei, L., D'Emilio, A., Falcieri, E., Piccoli, G., Agostini, D., Annibalini, G., Paolillo, M., Gioacchini, A. M., and Stocchi, V. (2009) Creatine

supplementation prevents the inhibition of myogenic differentiation in oxidatively injured C2C12 murine myoblasts. *Mol Nutr Food Res* **53**, 1187-1204

78. Buck, M., and Chojkier, M. (1996) Muscle wasting and dedifferentiation induced by oxidative stress in a murine model of cachexia is prevented by inhibitors of nitric oxide synthesis and antioxidants. *EMBO J* **15**, 1753-1765
79. Fulle, S., Protasi, F., Di Tano, G., Pietrangelo, T., Beltramin, A., Boncompagni, S., Vecchiet, L., and Fano, G. (2004) The contribution of reactive oxygen species to sarcopenia and muscle ageing. *Experimental gerontology* **39**, 17-24
80. Guttridge, D. C., Mayo, M. W., Madrid, L. V., Wang, C. Y., and Baldwin, A. S., Jr. (2000) NF-kappaB-induced loss of MyoD messenger RNA: possible role in muscle decay and cachexia. *Science* **289**, 2363-2366
81. Wang, H., Hertlein, E., Bakkar, N., Sun, H., Acharyya, S., Wang, J., Carathers, M., Davuluri, R., and Guttridge, D. C. (2007) NF-kappaB regulation of YY1 inhibits skeletal myogenesis through transcriptional silencing of myofibrillar genes. *Mol Cell Biol* **27**, 4374-4387
82. Powers, S. K., Duarte, J., Kavazis, A. N., and Talbert, E. E. (2010) Reactive oxygen species are signalling molecules for skeletal muscle adaptation. *Experimental physiology* **95**, 1-9
83. Kefaloyianni, E., Gaitanaki, C., and Beis, I. (2006) ERK1/2 and p38-MAPK signalling pathways, through MSK1, are involved in NF-kappaB transactivation during oxidative stress in skeletal myoblasts. *Cell Signal* **18**, 2238-2251
84. Barbieri, E., and Sestili, P. (2012) Reactive oxygen species in skeletal muscle signaling. *J Signal Transduct* **2012**, 982794

Figure legends

Fig 1. Iron content, oxidative stress, MAPKs phosphorylation, and satellite cell markers in mice models of aging, diabetes, and chronic kidney disease (CKD)

(A) Iron content of skeletal muscle in 2-month-old versus 2-year-old mice, *db/m* mice versus *db/db* mice, and control mice versus CKD mice. Values are expressed as mean ± SD. **P* < 0.05 (in each paired comparison); n = 8 in each group. (B) Left panel: Representative images of DHE staining of skeletal muscle of 2-month-old versus 2-year-old mice, *db/m* mice versus *db/db* mice, and control mice versus CKD mice with negative controls in each mouse (NC: negative control). Right panel: Quantitative analysis of relative fluorescence intensity. Values are expressed as mean ± SD; n = 5 in each group. **P* < 0.05 (in each paired comparison). (C) mRNA expression of the satellite cell markers *Pax-7*, *MyoD*, and *Myf5* in skeletal muscle of 2-month-old versus 2-year-old mice, *db/m* mice versus *db/db* mice, and control mice versus CKD mice. Values are expressed as mean ± SD; n = 5 in each group. **P* < 0.05 (in each paired comparison). Phosphorylation of (D) p38MAPK and (E) ERK1/2 in skeletal muscle of 2-month-old versus 2-year-old mice, *db/m* mice versus *db/db* mice, and control mice versus CKD mice. Upper panel: representative protein expression levels of phosphorylated p38MAPK, total p38MAPK, phosphorylated ERK1/2, total ERK1/2, and tubulin. Lower panels: semi-quantitative densitometry analysis of p38MAPK and ERK1/2 phosphorylation. Values are expressed as mean ± SD. **P* < 0.05 (in each paired comparison); n = 5 in each group.

Fig 2. Iron status, oxidative stress, MAPK phosphorylation, and satellite cell marker levels, and histology of skeletal muscle at basal conditions in mice with vehicle treatment or iron overload.

(A) Iron concentration in skeletal muscles. Values are expressed as mean ± SD. $^{**}P < 0.01$; n = 6–12 in each group. (B) Protein expression of H-ferritin (FTH) and L-ferritin (FTL) in skeletal muscle. Upper panel: representative protein expression levels of FTH, FTL, and tubulin. Lower panels: semi-quantitative densitometry analysis of FTH and FTL expression. Values are expressed as mean ± SD. $^{**}P < 0.01$; n = 6–9 in each group. (C) Left panel: Representative images of DHE staining of skeletal muscle with negative controls in each mouse. Right panel: Quantitative analysis of relative fluorescence intensity. Values are expressed as mean ± SD; n = 6–9 in each group. $^{**}P < 0.01$ (vs. vehicle). (D) Malondialdehyde concentration in skeletal muscle. Values are expressed as mean ± SD; n = 11–12 in each group. $^{*}P < 0.05$. (E) mRNA expression of satellite cell markers in skeletal muscle. Values are expressed as mean ± SD; n = 10–14 in each group. $^{**}P < 0.01$ (vs. vehicle). (F) Left panels: Representative images of Pax-7 (red), 4′,6-diamidino-2-phenylindole (DAPI, blue), and merged (purple) with negative control in gastrocnemius muscle of vehicle-treated and iron-treated mice. Right panel: Quantitative analysis of Pax-7 positive cells. Values are expressed as mean ± SD; n = 5-6 in each group. $^{*}P < 0.05$ (vs. vehicle). (G) Left panel: Representative images of skeletal muscle with or without iron load. Right panel: The mean area of muscle fibers.

Values are expressed as mean ± SD. (H) mRNA expression of atrogen-1 and MuRF1 in skeletal muscle. Values are expressed as mean ± SD; n = 7 in each group. (I) Left panels: Representative images of RhoNox-1 (red), hydroxyphenyl fluorescein (HPF, green), 4′,6-diamidino-2-phenylindole (DAPI, blue), and merged (orange) with negative control in gastrocnemius muscle of vehicle-treated and iron-treated mice. Right panel: Semi-quantitative analysis of RhoNox-1 and HPF fluorescence intensity. Values are expressed as mean ± SD; n = 5 in each group. *$P < 0.05$ (vs. vehicle).

Fig 3. Regeneration of skeletal muscle after cardiotoxin (CTX)-induced injury in mice with or without iron treatment

(A) The effect of iron overload on the changes in *myogenin* and *Myh3(eMyh)* mRNA expression in skeletal muscle after CTX injection. Values are expressed as mean ± SD. *$P < 0.05$, **$P < 0.01$ (vs. vehicle at same day); n = 6-14 in each group. (B) Left; Representative images of CTX-induced muscle injury at day 7 with or without iron loading. Right; The percentage of regenerating myofibers with centralized nuclei, the mean area of muscle fibers, and the distribution of myofiber areas in skeletal muscles 7 days after CTX injection. Values are expressed as mean ± SD. ** $P < 0.01$ (vs. vehicle); n = 6–14 in each group. (C) Left; Representative images of CTX-induced muscle injury at day 15 with or without iron loading. Right; Percentage of regenerating myofibers with centralized nuclei, the mean area of muscle fibers, and the distribution of myofiber areas in skeletal muscles at 15 days after CTX injection. Values are expressed as mean ± SD. ** $P < 0.01$ (vs. vehicle); n = 5-6 in each group. (D) The effect of iron overload

on changes in *Collagen 1a1* (*Col1a1*), *Collagen 1a2* (*Col1a2*), and *Collagen III* (*Col3a1*), and *Transforming growth factor beta-1* (*Tgf-β1*) mRNA expression in skeletal muscle after CTX injection. Values are expressed as mean ± SD. **P* < 0.05 (vs. vehicle at same day); n = 6 in each group. (E) Histological analysis of fibrosis in skeletal muscle at day 15 after CTX injury. Left; Representative images of picrosirius red staining in CTX-induced muscle injury at day 15 with or without iron loading. Right; Percentage of fibrosis fraction in skeletal muscles at 15 days after CTX injury. Values are expressed as mean ± SD. ** *P* < 0.01 (vs. vehicle); n = 5-6 in each group. (F) The effect of iron overload on the alteration in p38 and ERK1/2 phosphorylation in skeletal muscles after CTX injection. Values are expressed as mean ± SD. **P* < 0.05, ** *P* < 0.01 (vs. vehicle at same day); n = 6-10 in each group.

Fig 4. Effect of iron on C2C12 myoblast differentiation

(A) Effect of iron on cell proliferation and death in C2C12 myoblast cells. Left: Myoblast proliferation with or without iron stimulation. Values are expressed as mean ± SD, n = 8 in each group. **P* < 0.05, ***P* < 0.01. Right: Myoblast death with or without iron stimulation. Values are expressed as mean ± SD, n = 8 in each group. **P* < 0.05. (B) Western blot images of myogenin, myosin heavy chain (Myh)3, FTH, FTL, and tubulin during myoblast differentiation. The changes in protein expression of myogenin and Myh3 with or without iron treatment during myoblast differentiation. Values are expressed as mean ± SD. **P* < 0.05, ** *P* < 0.01; n = 16 in each group. (C) Effect of

iron on fusion index. Left: Representative immunohistochemical fluorescence of Myh3 (green) and DAPI (blue) in C2C12 myoblast cells. Right: Semi-quantitative analysis of fusion index. Values are expressed as mean ± SD. $^{**}P < 0.01$; n = 7 in each group. (D) The effect of iron on the alteration of p38 and ERK1/2 phosphorylation during C2C12 myoblast differentiation. Values are expressed as mean ± SD. $^{*}P < 0.05$, $^{**}P < 0.01$; n = 7–8 in each group.

Fig 5. The effect of tempol on iron-mediated suppressive effect on C2C12 myoblast differentiation

(A) Iron content of C2C12 myoblast cells. Values are expressed as mean ± SD. $^{*}P < 0.05$, $^{**} P < 0.01$; n = 6 in each group. (B) Iron-induced intracellular oxidative stress of C2C12 myoblast cells with or without tempol. Values are expressed as mean ± SD. $^{**} P < 0.01$; n = 12-18 in each group. (C) The effect of tempol on the suppression of muscle differentiation induced by iron. Values are expressed as mean ± SD. $^{*}P < 0.05$, $^{**}P < 0.01$ (vs. other 3 groups at same day); n = 12-16 in each group. (D) The effect of tempol on iron-mediated suppression of fusion index. Values are expressed as mean ± SD. $^{*}P < 0.05$, $^{**}P < 0.01$; n = 7 in each group. (E) The effect of tempol on iron-mediated reduction of p38MAPK and ERK1/2 phosphorylation. Values are expressed as mean ± SD. $^{*}P < 0.05$, $^{**}P < 0.01$ (vs. Fe+Tempol at same time); n = 8 in each group. (F) p38MAPK activity at 0 and 5 min after change in differentiation medium in C2C12 myoblast cells with or without iron treatment. Values are expressed as mean ± SD. $^{*}P <$

0.05, **P < 0.01; n = 7 in each group. (G) p38MAPK activity at 5 min after change of differentiated medium in iron-treated C2C12 myoblast cells with or without tempol. Values are expressed as mean ± SD. *P < 0.05 (vs. Fe); n = 7 in each group.

Figure 1 Ikeda, et al.

Figure 1

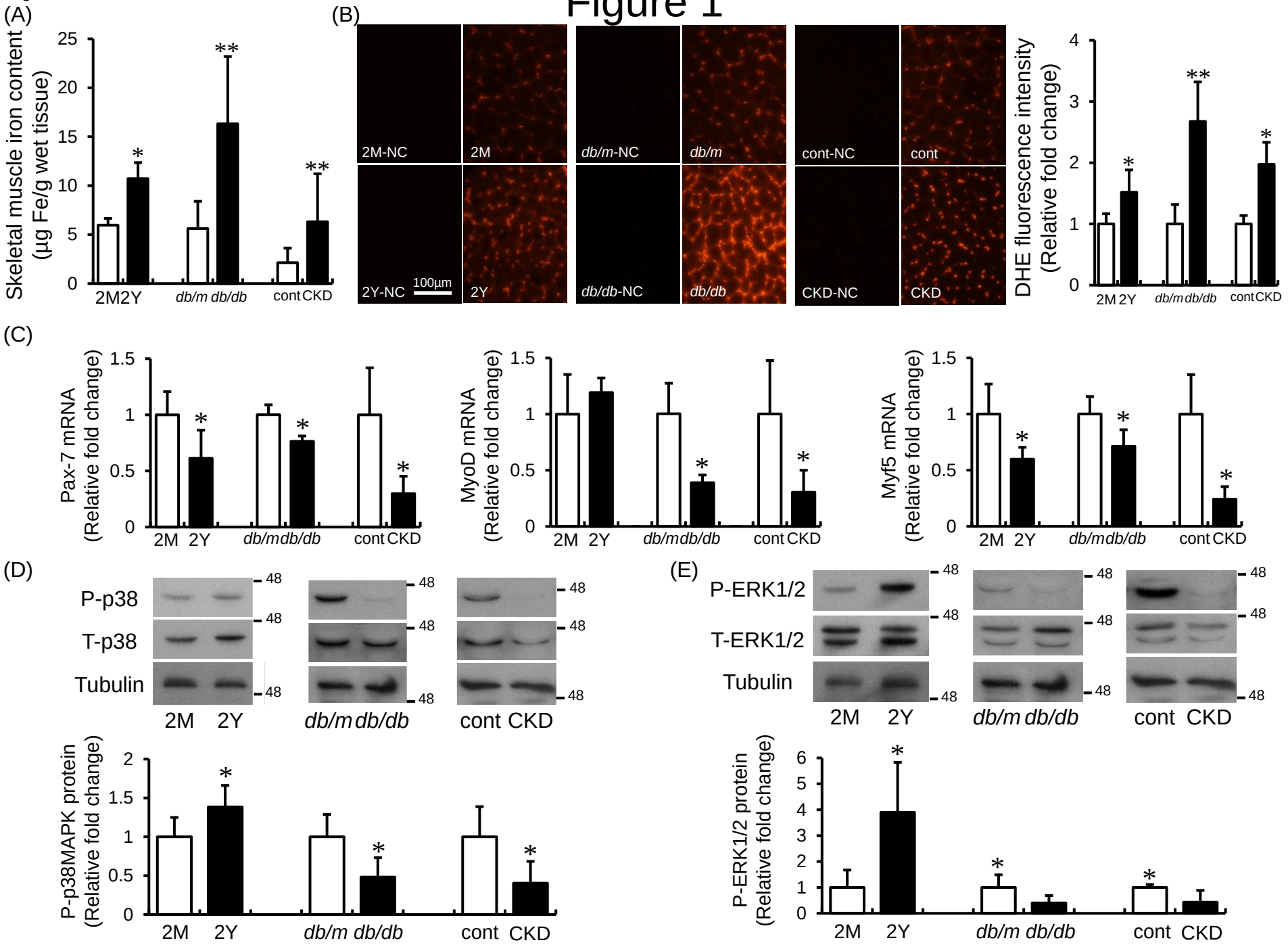

Figure 2 Ikeda, et al.

Figure 2-4

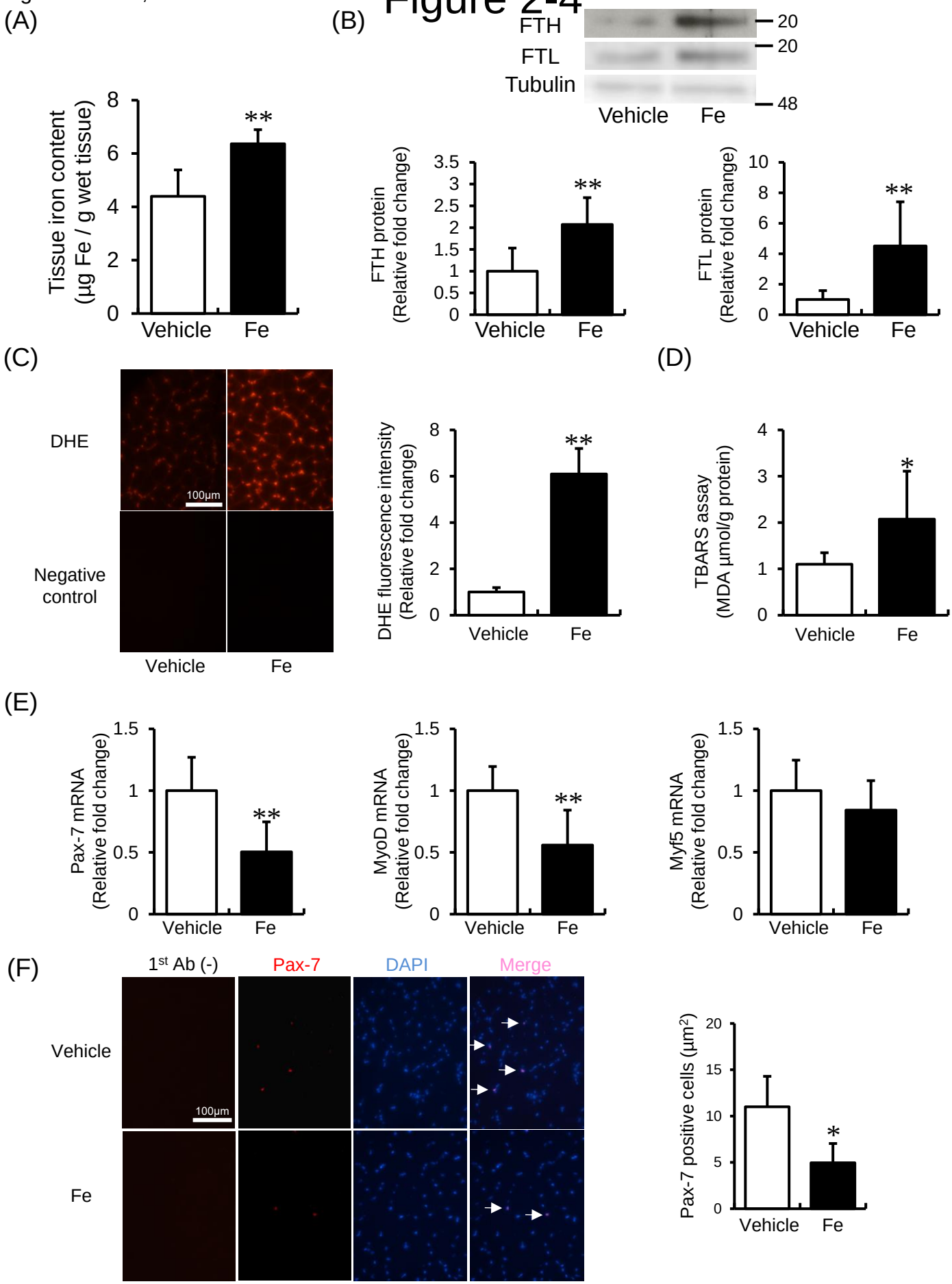

Figure 2 continued

Figure 2-4

(G)

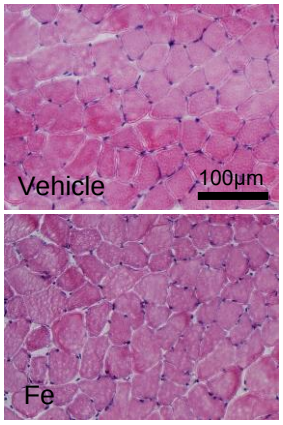

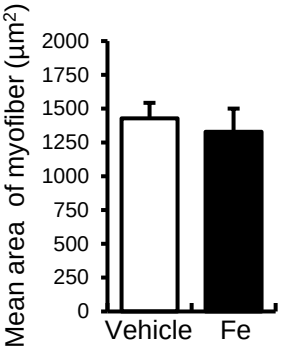

(H)

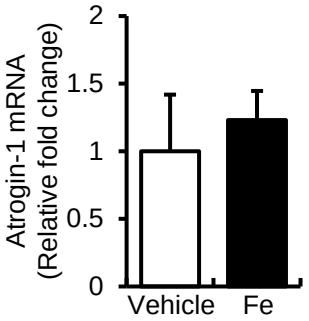

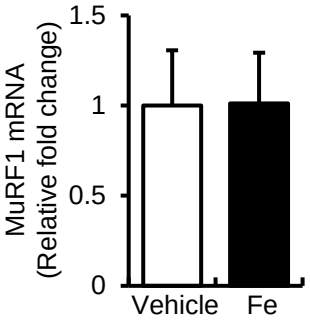

(I)

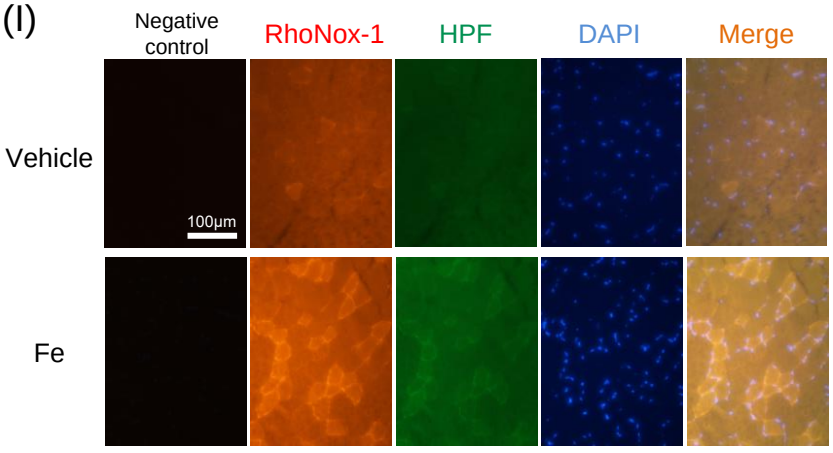

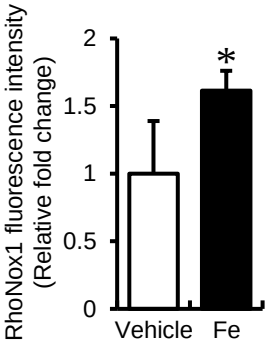

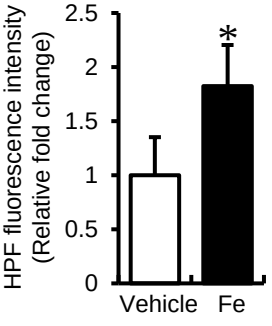

Figure 3 Ikeda, et al.

Figure 2-4

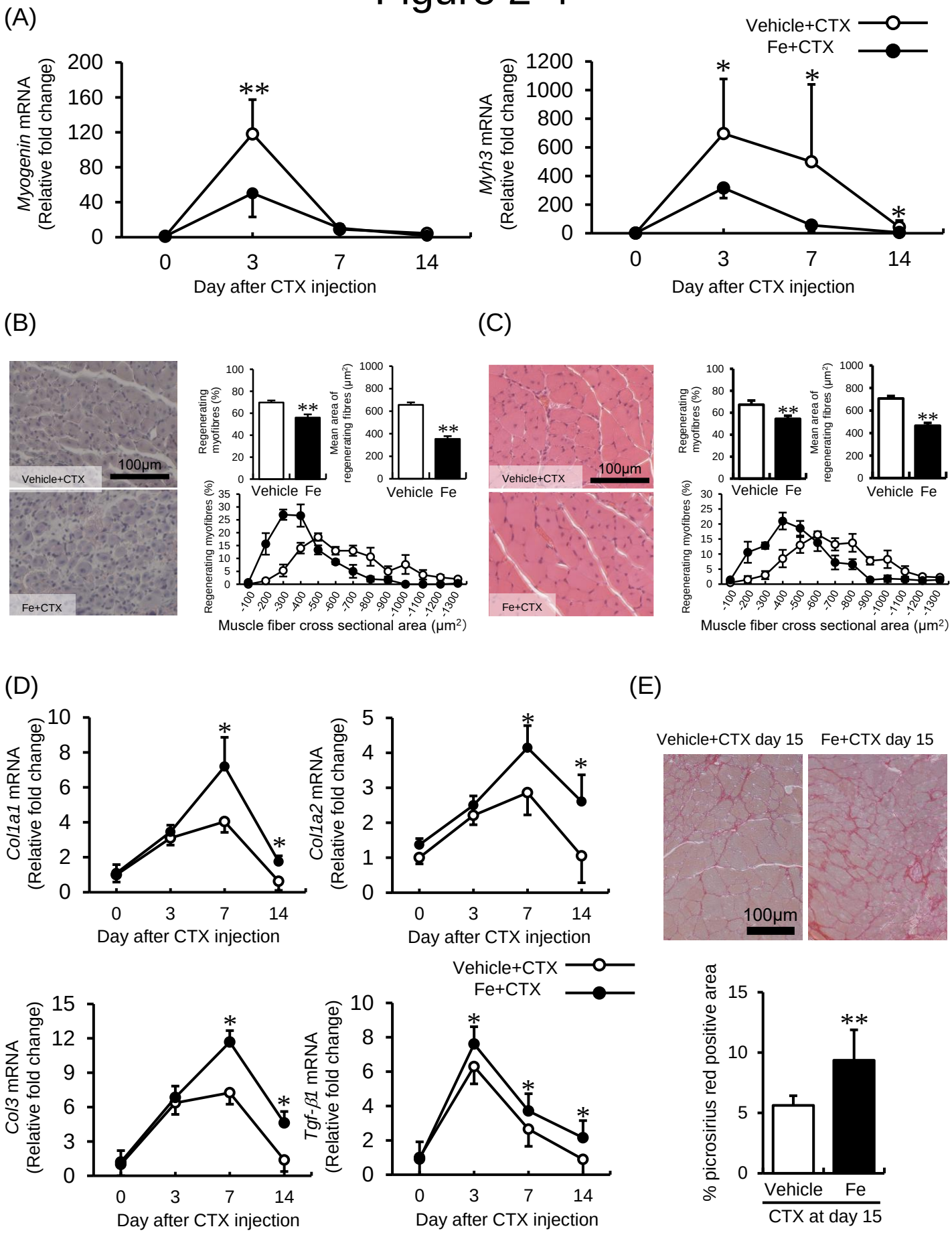

Figure 3 continued

Figure 2-4

(F)

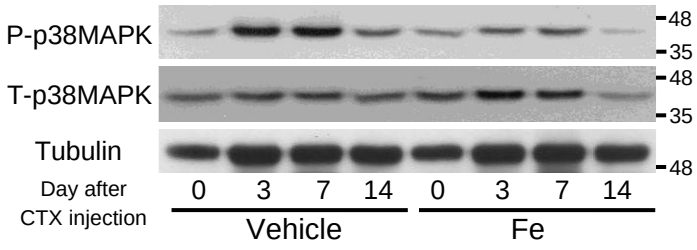

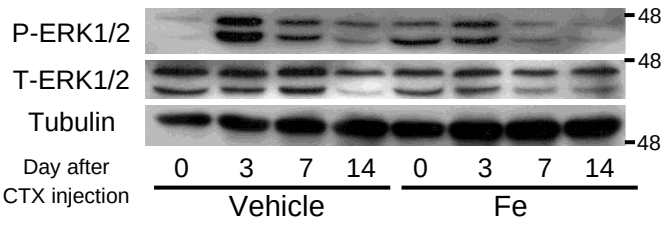

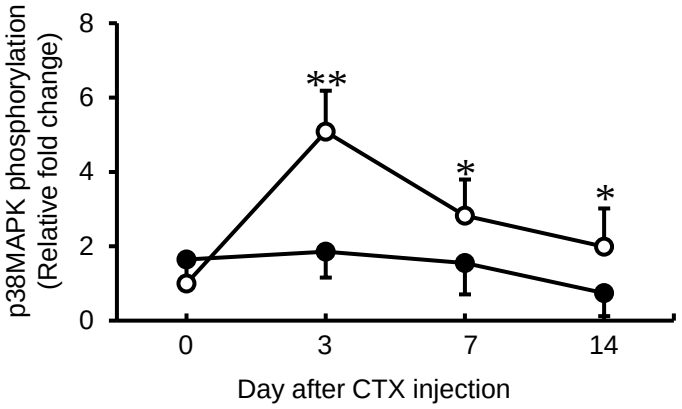

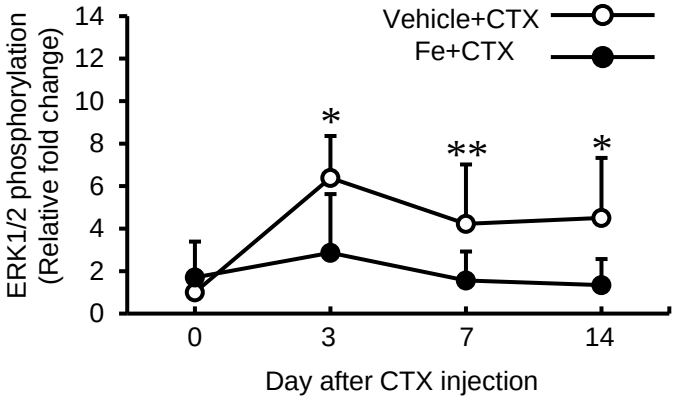

Figure 4 Ikeda, et al.

Figure 2-4

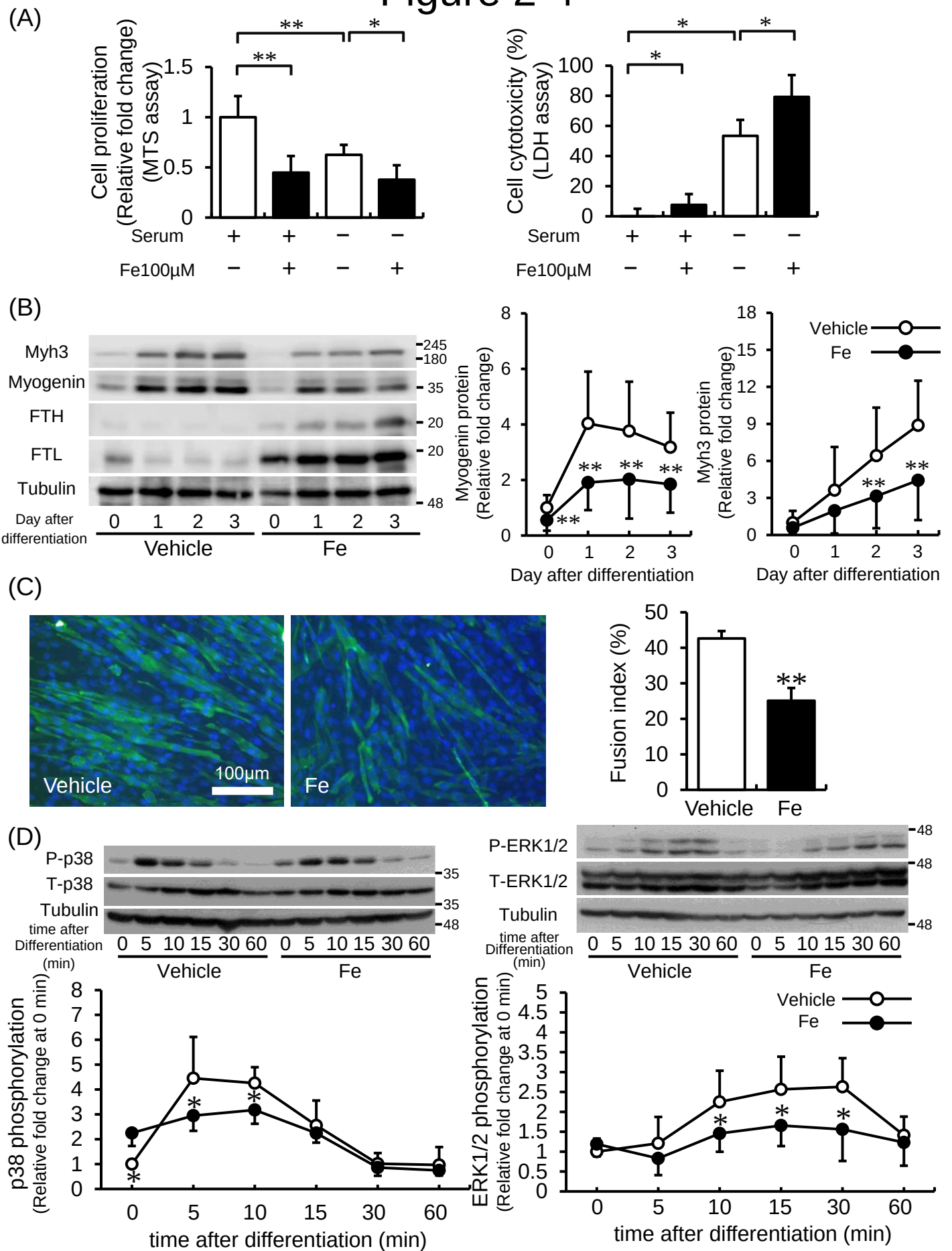

Figure 5 Ikeda, et al.

Figure 5

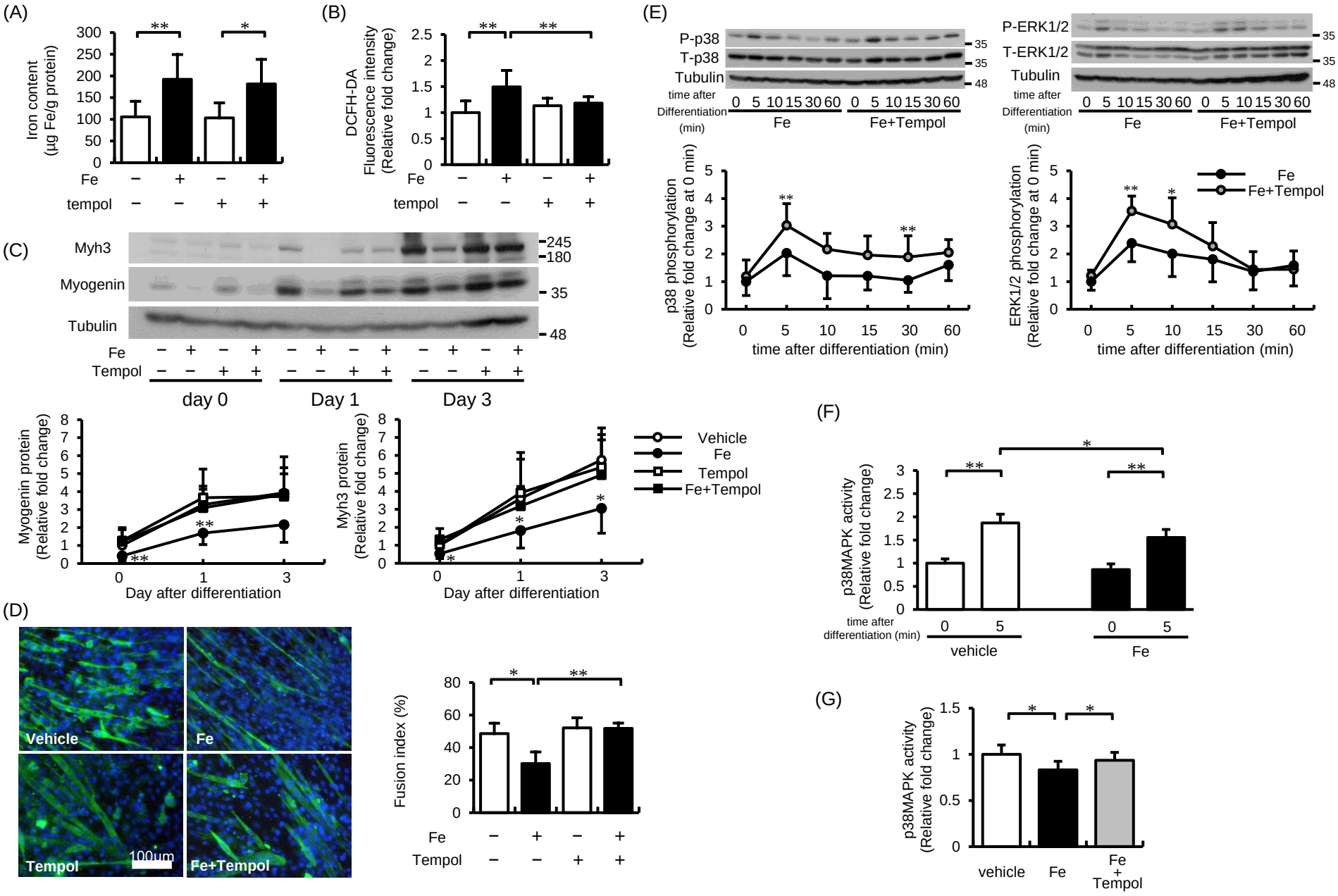

Table 1. Characteristics of vehicle-treated mice and chronic iron-treated mice

	Vehicle-treated group	Iron-treated group
Initial body weight (g)	20.9 ± 1.3	20.9 ± 0.8
Body weight 4 weeks later (g)	24.9 ± 2.9	24.2 ± 1.5
Gastrocnemius muscles (mg)	141.2 ± 20.0	136.4 ± 8.9
Soleus muscles (mg)	9.2 ± 1.2	9.0 ± 1.3
Extensor digitorum longus muscles (mg)	14.4 ± 1.4	13.7 ± 0.9

Values are expressed as mean ± SD. n = 5-14 in each group.

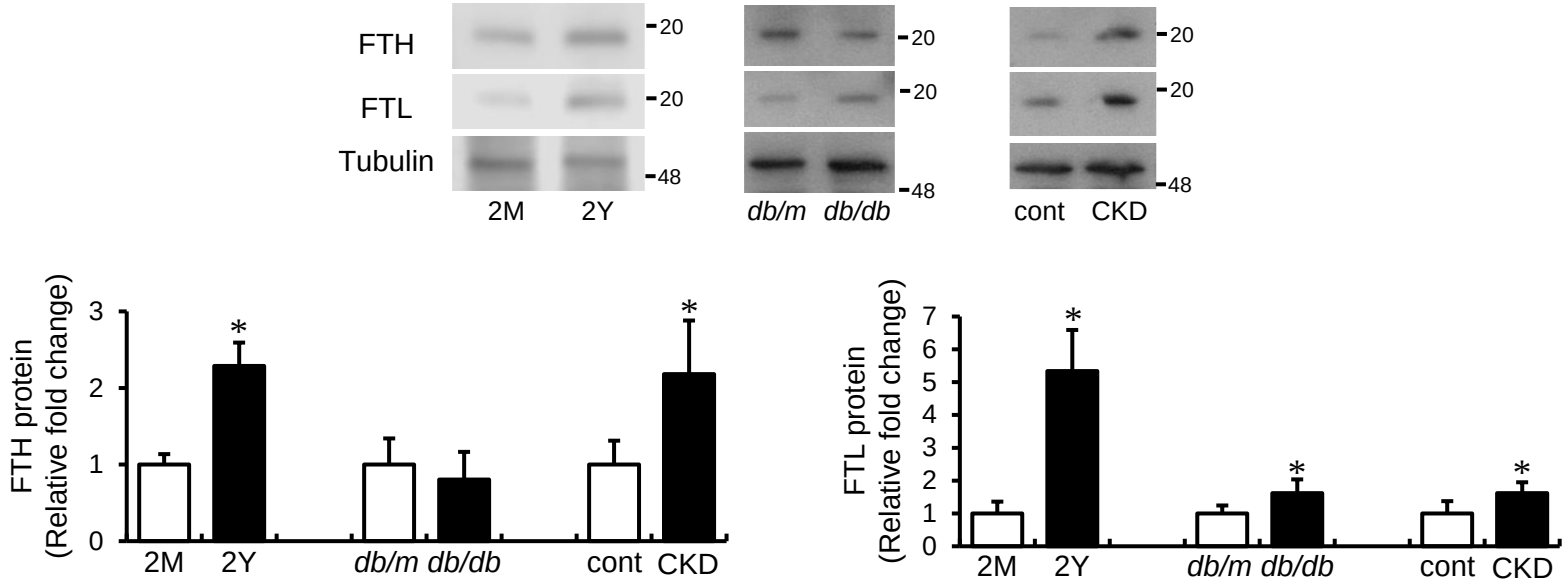

Supplementary figure 1

Protein expression of H-ferritin (FTH) and L-ferritin (FTL) in skeletal muscle of 2-month-old and 2-year-old mice, *db/m* mice and *db/db* mice, and control mice and CKD mice. Upper panel: representative protein expression levels of FTH, FTL, and tubulin. Lower panels: semi-quantitative densitometry analysis of FTH and FTL expression. Values are expressed as mean ± SD. **P* < 0.05 (vs. 2 months of age, *db/m* mice, and control mice in each); n = 5 in each group.

Supplementary Figure 2 Ikeda, et al.

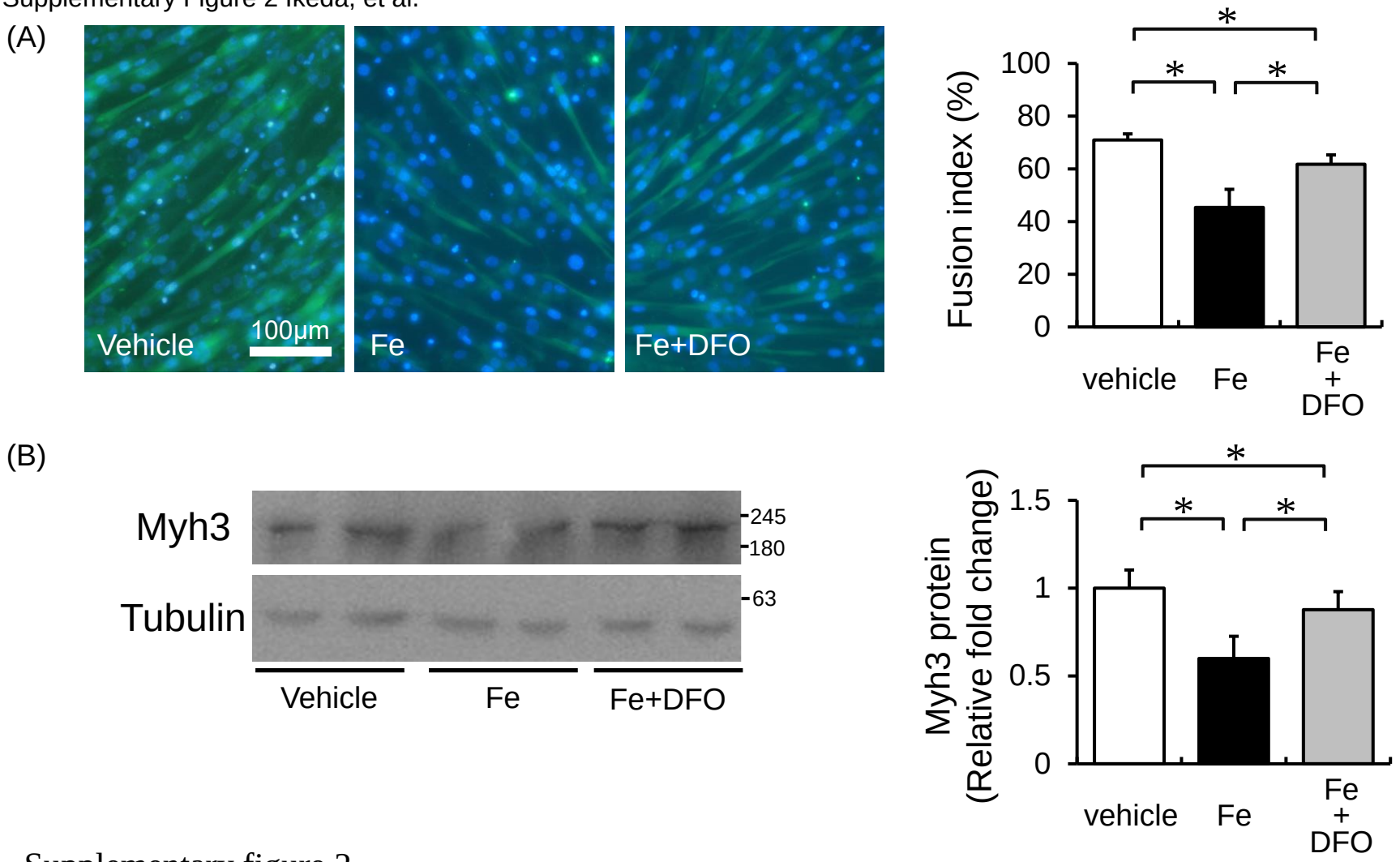

Supplementary figure 2

The effect of deferoxamine (DFO) on iron-mediated suppression of myoblast differentiation. (A) Effect of iron on fusion index. Left: Representative immunohistochemical fluorescence of Myh3 (green) and DAPI (blue) in C2C12 myoblast cells. Right: Semi-quantitative analysis of fusion index. Values are expressed as mean ± SD. *$P < 0.05$; n = 5 in each group. (B) Western blot images of myosin heavy chain (Myh)3, and tubulin during myoblast differentiation. Values are expressed as mean ± SD. *P < 0.05; n = 5 in each group.